



Estimation of Pore Volume Compressibility in Carbonate Reservoir Rocks Based on a Classification

Seyed Amin Moosavi  · Hesam Aloki Bakhtiari · Javad Honarmand

Received: 15 April 2021 / Accepted: 20 February 2022 / Published online: 7 March 2022
© The Author(s), under exclusive licence to Springer Nature Switzerland AG 2022

Abstract This study examined the petrographically classification, petrological and petrophysical characteristics by taking a vast range of carbonate reservoir rock from Asmari and Bangestan group Formations in southern Iran basins. Implications of these characteristics were also studied to estimate the pore volume compressibility of the carbonate reservoirs. In the current study, a method is developed to classify the carbonate reservoir rocks based on the dominant factors involved in elastic properties of pore volumes. For classification, several 3702 thin sections were studied. Then, the pore volume compressibility of 200 core plugs corresponding to the range of classification parameters was obtained and quantified by a pre-proven equation. Based on the studied classification, the results clearly show an acceptable narrow bandwidth between the upper and lower bound of estimations. Furthermore, the analysis of the pore compressibility–stress relationship was in good agreement with the experimental observations. Also, the study shows that integrating the routine petrophysical properties is helpful for the estimation of stress-related properties of pore volumes into carbonate reservoir rocks.

Keywords Pore volume compressibility · Classification · Porosity · Permeability · Stress

1 Introduction

Pore volume compressibility (PVC) of carbonate reservoirs is essential factor for characterizing coupled fluid transport and stress. Therefore, PVC is of particular interest to the petroleum industry, especially for wells' design, drilling and completion, production forecasts, and material balance studies.

Hydrocarbon production operations can cause reservoir compaction due to reduced pore fluid pressure and subsequent changes in external effective stress (Geertsma 1957). To study reservoir compaction, it is necessary to know the compressibility characteristics of the reservoir rock. Pore volume compressibility (PVC) is one of the most common types of compressibility of porous media (Teeuw 1971). The PVC of reservoir rock is usually measured by the change in pore volume at different pore pressure levels in the laboratory. In most cases, laboratory determination of PVC has encountered some problems due to difficulty in acquiring accurate core samples and time consuming and costly sample preparation procedures. In other situations, sometimes, the lack of appropriate core samples from the reservoir is another challenge that may be encountered in obtaining an accurate value for PVC. So, several researchers have proposed empirical relation to estimate PVC (Chuanliang et al.

S. A. Moosavi (✉)
Mining Engineering Department, Vali-E-Asr University
of Rafsanjan, Rafsanjan, Iran
e-mail: aminmoosavi@vru.ac.ir

H. A. Bakhtiari · J. Honarmand
Research Institute of Petroleum Industry, Theran, Iran

2004; da Silva et al. 2015; Hall 1953; Harari et al. 1995; Horne 1997; Jalalh 2006a, b; Newman 1973). Based on experimental measurements, Hall (1953) proposed a simple inverse equation between PVC and porosity. To evaluate the accuracy of the PVC models previously published by Hall (1953), van der Knaap (1959), Horne (1997), and Jalalh (2006b), in an experimental study da Silva et al. (2015) investigated the petrophysical properties of carbonate rocks from North America from three distinctive geologic backgrounds. They presented better accuracy of the Jalalh (2006b) model to that of Hall (1953) as a function of porosity.

The main shortcoming of these equations was the influence of rock lithology, which had not taken place, and for different lithologies with the same porosity, the same value for PVC was proposed. However, pore volume compressibility of reservoir rock is related not only to porosity but also to elastic properties of the constituents, which are affected by the microstructural petrological characteristics as well. The porous rock's macroscopic properties are closely related to its microstructural features. Different researchers have shown the effect of microstructure on macroscopic properties of rock, such as elasticity, bulk modulus, compressibility, and permeability. So, to deal with this issue, some studies have been published on the relationship between PVC and mineralogy of different consolidated and unconsolidated rock Formations, such as Newman (1973), Zimmerman (1991), Harari et al. (1995), and (Horne, 1997). Horne (1997) has proposed three nonlinear relationships between initial porosity and PVC for consolidated and unconsolidated sandstones and consolidated limestones.

However, except for simple cases of reservoir management, a universal relation between PVC and stress for different rock types is required. Therefore, some studies have developed some stress-related pore compressibility for reservoir rocks mainly based on experimental approaches. Harari et al. (1995) have worked on four limestone lithologies from Saudi Arabian basins under the condition of hydrostatic differential stresses to study pore compressibility at constant pore pressure. They showed that a power-law equation is appropriate to evaluate differential stress-related pore compressibility at constant pore pressure. Also, they found that the sensitivity of pore compressibility at lower stress values is higher than it at higher stress conditions. Based on their study, no distinct

and universal relation was found because the theoretical background to support the idea of the selection of regression formula was not declared. However, the validity of their model is acceptable for qualitative and comparison studies associated with rock samples from Saudi Arabian basins. Oliveira et al. (2016) have shown a power-law fit suitable for the PVC vs. confining pressure experimental data. But, differently, Liu et al. (2009) have derived two universal theoretical formulations for pore and bulk compressibilities of rocks using a novel conceptualization of the heterogeneous rock in two distinct parts, one part follows a natural-strain-based Hooke's law, and the other part obeys an engineering-strain-based Hooke's law. Consequently, they proposed a universal exponential equation for the PVC–stress relationship as follows:

$$C_{pc} = C_{pc}^{\infty} + \frac{\gamma}{\phi_0 K} \exp\left(-\frac{\sigma}{K}\right) \quad (1)$$

where, C_{pc} is the pore compressibility, σ is the hydrostatic confining stress, ϕ_0 is unstressed initial porosity, and C_{pc}^{∞} , γ , and K are constants that can be evaluated by fitting the equation on experimental data points.

Based on the concept proposed by Liu et al. (2009), more studies were done by Wang et al. (2009), Moosavi et al. (2014), Zheng et al. (2016), Liu et al. (2016), and Rinaldi and Rutqvist (2019). They have studied other stress-related petrophysical characteristics of rocks. These studies have examined the robustness of the mathematical exponential expression and its ability to prove porosity–stress and permeability–stress relations. Furthermore, some other researchers worked on the complexity of experimental evaluation of PVC in specific reservoir conditions (Zheng and Espinoza 2021), digital image processing based simulations to study the effect of pore structure geometry on rock compressibility (Sui et al., 2020), and analytically modelling of PVC (Lei et al. 2019; Zhu et al. 2018). All these studies have focused on the effects of geometry and its related complexities and have not addressed the importance of lithological structure.

However, research on the PVC of carbonate reservoirs and the effect of its geological characteristics, despite its great importance, is limited worldwide, especially in Iran. Although few researchers have studied the PVC of reservoirs in recent years, there

are still ambiguities and complexities in this regard. In the current research, considering various parameters affecting PVC in samples of two of the most important carbonate reservoirs (Asmari and Bangestan) in five of Iranian major oil fields, the relationship between these parameters and PVC in carbonate reservoirs has been investigated.

Accordingly, in the present study, because of its proven capability in the literature for fitting the stress-related PVC data points, the mathematical concept of Eq. (1) was selected to interpret the experimental observations. To categorize and classify the pore volumetric changes of carbonate rocks under stress variation, about 200 core plug samples were collected from Asmari and Bangestan reservoir horizons in southern Iran. Asmari (Oligo-Miocene in age) and Bangestan (Late Albian-Turonian in age) reservoir Formations, deposited in Zagros foreland basin, together have the largest share in oil storage and production in Iran and therefore the most available data. Porosity, permeability, grain density measurements as well as detailed petrographical studies were done for all of the selected thin section samples. But, before sample selection for testing, an extensive petrographical study was performed to classify the samples based on the geological aspect of which carbonates are the dominant ones on microphysical properties of the porous media. Therefore, petrographical studies were done on 3306 thin sections from the Asmari Formation collected from key wells in Maroon, Rag Sefid, Gachsaran, Bibi Hakimeh, and Aghajari oilfields and 396 thin sections from Bangestan reservoir horizon of Maroon and Rag-Sefid oilfields. But due to uncertainty in some samples, several thin-section samples were removed from the analysis process in the geological classification.

The main objective of this paper is to find out a relationship between the pore volume compressibility and geological characteristics of carbonate rocks. Even though many researchers were worked on the pore volume compressibility of rocks for different lithology, very few researchers were studied the pore volume compressibility as complete stress related curve, quantitatively. Therefore, in addition to the lithological study of a large number of thin sections and the determination of a classification based on the porosity–permeability frequency, a quantitative correlation has been provided that makes it possible to estimate the compressibility–stress curve, completely

(not as a single value). These quantitative estimations were based on the coefficients of a pre-proven mathematical equation. Validity and robustness of the equation were also proved by testing a large number of core rock samples. Therefore, according to this study, without performing compressibility tests, the complete PVC–stress curve can be estimated based on the lithological characteristics of the carbonate reservoir rock, which can be used in reservoir engineering studies.

This paper is organized as follows. First, the investigation of the main effective petrographic characteristics of carbonate reservoir rocks that significantly affect the behavior of the porous rocks under stress regimes is presented. Moreover, an appropriate lithological–textural classification was proposed based on the frequencies of the important aspects. Then, in the second part of the study, experimental tests were performed on the 200 corresponding core plug samples. The experimental tests included porosity, permeability, and pore volume compressibility determination. The PVC-stress curves were fitted on the aforementioned mathematical equation to determine the corresponding fitting constants. Comparisons were then made between these experimentally driven constants as full description indices of volumetric changes due to stress change and rock classification.

2 Petrographic Studies and Rock Typing

Different rock typing methods have been developed to categorize reservoir rocks into petrophysical units based on geological characteristics (Dou et al. 2011; El Sawy et al. 2020). Previous studies have shown the importance of lithology/mineralogy, texture, and porosity on the pore compressibility of reservoir carbonate rocks (Aloki Bakhtiari et al. 2011; Lis-Śledziona, 2019; Satter and Iqbal 2016; Sui et al. 2020). The selection of the rock typing method with the aim of sample selection for further experimental tests requires an adequate understanding and to distinguish between different classification criteria. But according to previous studies, lithology, texture, and amount and type of porosity are the most important parameters controlling the pore compressibility of carbonate rock. Therefore, the best method for classifying carbonate rocks would be to consider all lithological, textural, and porosity boundaries are

Table 1 Parameters described in the petrographic studies

Well	Depth	Lithology	Mineralogy		Anhydrite (%)			Visual porosity (%)			Core Permeability								
			Calcite	Dolomite	Anhydrite	Quartz	Texture	Nodule	Cement/Replacement	Interparticle		Intercrystalline	Moldic/Intraparticle	Vuggy	Total	Core Porosity			

considered. A brief explanation of some routine classification methods is provided to identify the different classifications of voids in carbonate rocks.

Archie (1952) was the first researcher to link rock fabric with petrophysical properties of carbonate rock in his classification. This skeleton classification with symbols is used to estimate petrophysical data, such as porosity, permeability, capillary pressure, and electrical conductivity. But since these descriptive features cannot be defined in sedimentary or diagenetic terms, it is difficult to relate them to geological models. Furthermore, the major problem is that no prediction has been made to distinguish visible interparticle spaces from other types of visible voids such as moldic porosity. However, the importance of the relationship between voids and sedimentary and diagenetic fabric and distinguishing between interparticle spaces and other types of voids has been shown (Choquette and Pray 1970; Lucia 1983; Murray 1960). Based on how the voids spaces are formed, Choquette and Pray (1970) divided all the carbonate voids into two major groups: fabric selective and non-fabric selective. According to this classification, moldic and intragranular voids are classified as fabric selective porosity and placed in the same group with interparticle and intercrystalline porosity. However, Lucia (1983) expressed that moldic and intragranular voids have different effects on petrophysical properties than interstitial and intercrystalline voids and should therefore be grouped separately. So, Lucia (1983) proposed a more general classification of carbonate porosity to be used in the carbonate rocks description. In their work, Lucia (1983) classified interparticle porosity based on the particle size and the dense or porous appearance of the interparticle area. Also, they classified vuggy porosity according to the type of interconnection. Separate vugs are defined as pore space interconnected only through interparticle pore space. In contrast, touching vugs are defined as ones that form an interconnected pore system independent of interparticle pore space. In this classification, separate vugs are typically fabric-selective in their origin. Intragranular and moldic pore spaces are examples of fabric-selective separate vugs. Touching vugs are typically nonfabric selective in origin. Cavernous, collapse breccia, fracture, and solution-enlarged fracture pore types commonly form an interconnected pore system on a reservoir scale and are typical touching-vug pore types.

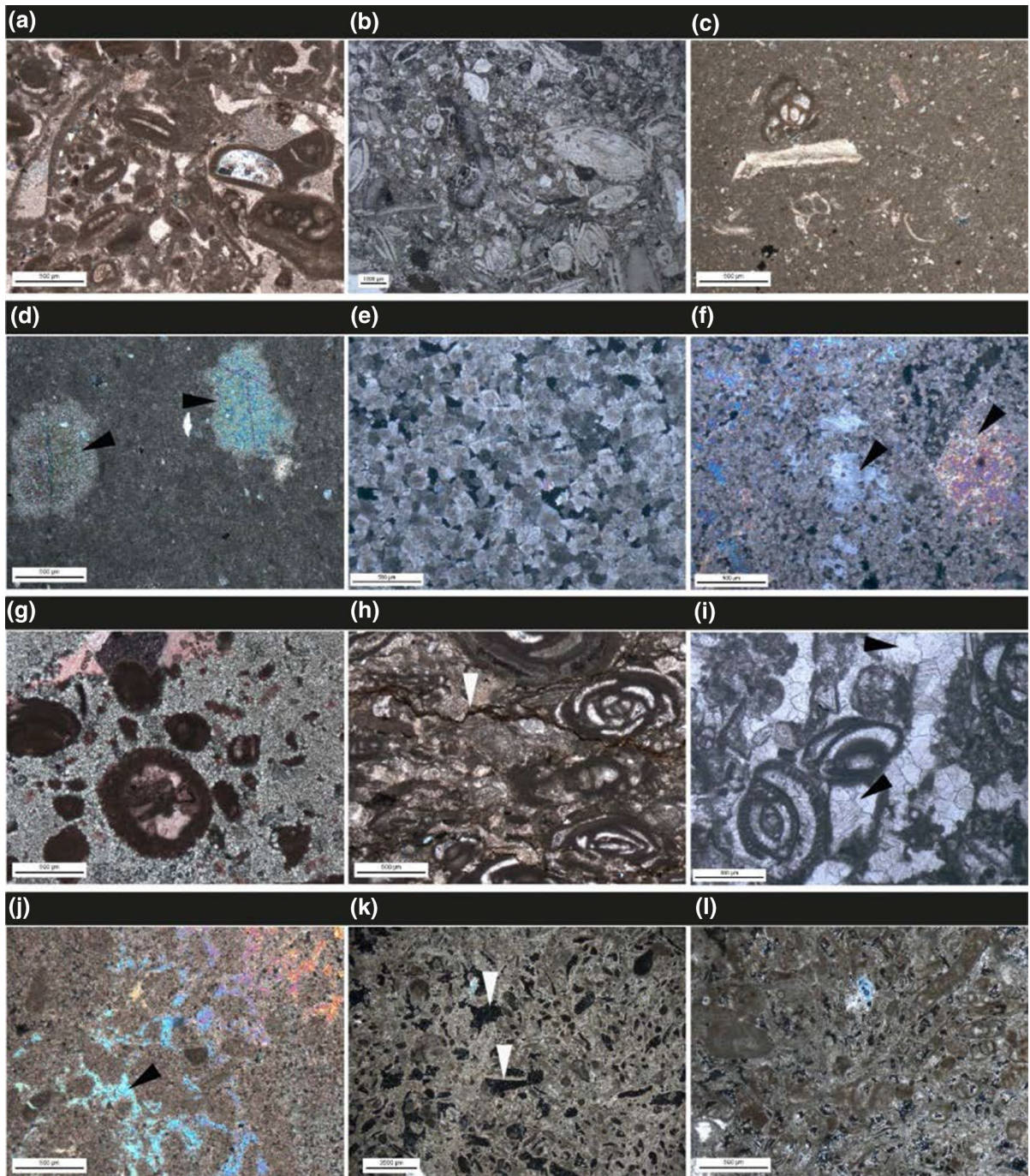


Fig. 1 Photomicrographs of the Asmari Formation in the studied fields. **a–d** showing different textures (**a** grainstone; **b** packstone; **c** wackestone; **d** mudstone with anhydrite nodules-arrows); **e–g** showing dolostone samples with different crystal size (**e** coarse crystalline; **f** medium crystalline with anhydrite

precipitation-arrows; **g** fine crystalline); **h** stylolite as a chemical compaction feature; **i** calcite cementation; **j** anhydrite precipitation in a fine crystalline dolopackstone; **k** dissolution porosities; **l** interparticle pore spaces in a skeletal grainstone

Fig. 2 Porosity–permeability cross plots with the most frequent data samples for **a** Limestone, **b** Dolostone

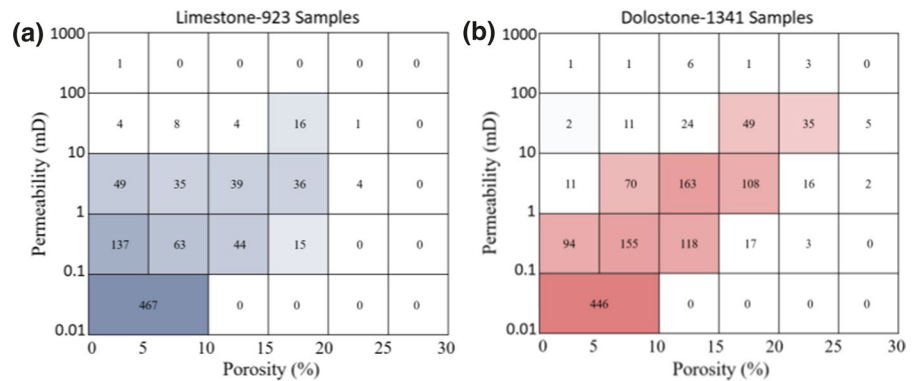


Fig. 3 The CMS-300 machine

In the present study, because of its comprehensiveness, the adequacy of Lucia (1983) carbonate classification was examined for use in the prediction of PVC for Asmari (Oligo-Miocene in age) and Bangestan group (Albian-Turonian in age) Formations. These Formations are the most important carbonate reservoir Formations in the hydrocarbon fields of the Zagros Basin, Iran. So, 3702 thin sections from these Formations (in 8 key wells) were selected. These samples were studied by polarizing microscope for selective geological parameters (Table 1) during petrographical studies. These thin sections were studied in detail for National Iranian South Oil Company (NISOC) by the geologist of this paper as a research project (Aloki Bakhtiari et al. 2014).

According to petrographic studies, the Asmari Formation was composed of dolostone and limestone from the lithological point of view. In contrast, due to very limited dolomitization, the Bangestan group Formation (Sarvak) was composed only of limestone. Geological studies of the Asmari Formation in the studied wells have shown that the reservoir quality of this Formation is not very dependent on its sedimentological characteristics, especially texture, and is mainly affected by various diagenetic processes that affect this Formation with different intensities and as a result, have changed lithology and reservoir properties (Fig. 1).

Diagenetic events, especially dolomitization, anhydrite precipitation, dissolution, and calcite cementation, are the main factors controlling the reservoir properties of the Asmari Formation. In Lucia's classification, this results in samples with the same texture as grainstone but with different porosity and permeability being classified the same (class 1). On the one hand, the placement of specimens with different textures such as mudstone, wackestone, and mud-dominated packstone and possibly different porosity and permeability in a class (class 3) also means that in the selection of samples based on Lucia classification, all parameters affecting compressibility are not considered. On the other hand, in the first stages of this study, the classification of carbonate samples and then sample selection, should not be entirely dependent on a petrographic parameter such as the texture or dolomite crystal size (as in the Lucia classification). Because core or thin-section samples may not be available in many reservoirs, relying on the grouping of petrographic parameters reduces the efficiency of that grouping. However, the type of porosity used in the Lucia classification is interparticle porosity, and

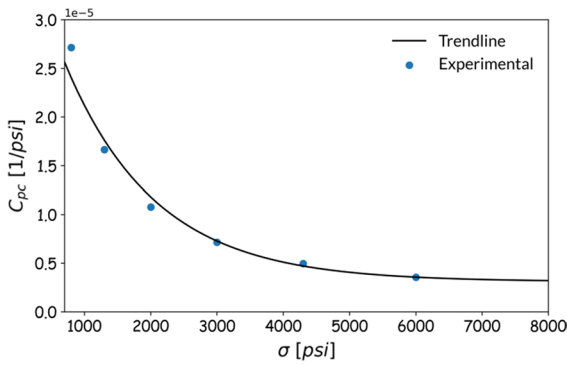


Fig. 4 PVC (C_{pc}) vs. confining stress (σ) for a sample (Sample No. 91)

other types of porosity such as vuggy and moldic types are not included in this diagram, although these pore spaces can also affect compressibility. So, pinning down the exact nature of the visual inspection of thin sections and choosing an appropriate classification based on the micro-observation could not lead us to similar trends in each corresponding class. Therefore, to select a suitable classification model, other influential characteristics should exist such that pore geometry and its complexity are also reflected. So, because the exact choice of the effective quantitative parameters was not applicable by thin section study due to the aforementioned reasons, a sufficiently rich grouping model via another setting of the characteristics was needed. However, it required a different class of models to deal with fundamentally different logical parameters; moreover, it should reflect the pore characterization that was not obtained by thin section-based parameters. Therefore, this study preferred to use the common reservoir classification (pore-perm cross plots) with particular attention to sedimentary texture, dolomite crystal size and the existing limitations of the device in measuring compressibility.

The porosity and permeability values represent pore geometry and complexity as well.

Hence, based on the core analysis results, porosity–permeability cross-plots of the studied samples in different lithologies, textures, and dolomite crystal sizes were prepared (Fig. 2). The relationship between geological features and reservoir properties in the studied samples, especially Asmari samples, was complex, which made selecting samples for compressibility tests difficult. For this reason, the parameters of lithology, porosity, permeability, and frequency of samples in each porosity–permeability cell were the basis for sample selection. The distribution of samples in porosity–permeability cross-plot is such that by considering a network of porosity and permeability with dimensions of 5% porosity and permeability of a logarithmic unit and considering the frequency, lithology, texture, and crystal size in each cell, sampling was performed.

3 Experimental Tests and Interpretation

The pore volume compressibility tests were performed by the CMS-300 (Fig. 3). The device has 12 core holders, such that in each series of tests, a maximum of 12 samples can be placed in the device. The pore fluid is helium gas, and the hydrostatic pressure can be provided by the device up to 10,000 psi under ambient temperature conditions. CMS-300 can measure porosity in the range of 0.01–40%, pore volume changes, gas permeability, Klinkenberg permeability (liquid equivalent permeability), and Forchheimer’s coefficients at stepwise increasing overburden pressures from 800 to 10,000 psi. The length of the cores can range between 0.75 inches to 4 inches. In this system, the pore volume is determined by Boyle’s law. Boyle’s law states that the volume of

Table 2 Data interpretation for a sample (Sample No. 91)

σ (psi)	ϕ (%)	k (md)	C_{pc} (psi^{-1})	C_{pc}^∞ (psi^{-1})	ϕ_0 (%)	γ (%)	K (psi)
800	17.1	0.327	2.71E-05	3.11E-06	17.5	0.899	1364.65
1300	17.0	0.313	1.67E-05				
2000	16.9	0.296	1.08E-05				
3000	16.7	0.277	7.16E-06				
4300	16.5	0.257	4.98E-06				
6000	16.4	0.237	3.55E-06				

gas decreases with pressure regularly. In other words, there is always an inverse relationship between volume and pressure at constant temperature. According to Boyle’s law, at a constant temperature, the value of PV is equal to nRT . Where, in these relations, P is the gas pressure, V is the volume of gas, n is the number of moles of gas, R is the global constant of gases and T represents the ambient temperature. The volume change can be calculated using Boyle’s law at a constant temperature. Helium gas is injected at the same temperature from the tank chamber with a specific volume at a certain pressure to the sample holder. After gas expansion, the equilibrium pressure is recorded to measure the pore volume, and the volume value is calculated using Boyle’s law.

Before placing the samples in the device, the dimensions of the sample and its initial porosity are measured and recorded under ambient pressure conditions. To determine the PVC using CMS-300, the

typical load on the core sample is hydrostatic (i.e., equal values of confining stress in all directions).

The recorded data from CMS-300 were processed to plot PVC vs. confining stress for different stress steps. Furthermore, using the Eq. (1), the trendline on the scattered processed data was matched automatically by a computer code. The coefficients of the trendline equation are summarized in the Table 5. Moreover, the interpretation of data for a sample is shown in Fig. 4 and Table 2, just as an example. Figure 4 shows the PVC vs. stress for a specific core sample which is selected randomly (sample No. 91). The exponential best fit was determined for this rock sample (and also for all of rock core samples that were tested). The scatter experimental data points and corresponding coefficients of the exponential trendline through this data points were summarized in Table 2. This trendline based on the Eq. (1) represent a very good and satisfactory for the experimental

Table 3 The values of coefficients C_{pc}^∞ , γ and K for limestone samples based on the classification of porosity–permeability frequent groups

ϕ_0	k_0	Lower bound			Upper bound			Average		
		C_{pc}^∞	γ	K	C_{pc}^∞	γ	K	C_{pc}^∞	γ	K
0–10	0.01–0.1	3.80	0.49	1286.67	9.07	0.79	1358.98	5.60	0.56	1333.19
0–5	0.1–1	3.20	0.28	1056.50	33.4	1.18	1799.10	11.97	0.73	1348.65
0–5	1–10	7.32	0.66	1168.92	10.53	0.96	1310.8	8.88	0.84	1253.89
5–10	0.1–1	3.04	0.38	1346.30	6.67	0.86	1360.84	5.16	0.65	1351.02
5–10	1–10	3.81	0.54	1307.98	10.5	1.01	1359.31	6.32	0.79	1353.87
10–15	0.1–1	2.15	0.48	1359.30	4.07	0.86	1366.36	3.14	0.64	1362.97
10–15	1–10	2.63	0.57	1357.07	5.21	1.12	1364.88	3.53	0.76	1362.09
15–20	0.1–1	1.57	0.51	1362.3	3.85	1.01	1368.13	2.59	0.74	1365.65
15–20	1–10	2.12	0.62	1356.88	5.87	1.53	1366.71	3.12	0.88	1364.49
15–20	10–100	2.58	0.76	1364.65	3.33	1.10	1366.09	2.99	0.92	1365.16

*Units: C_{pc}^∞ [$\times 10^{-6}$ psi $^{-1}$], γ and ϕ_0 [%], k_0 [mD], and K [psi]

Table 4 The values of coefficients C_{pc}^∞ , γ and K for dolostone samples based on the classification of porosity–permeability frequent groups

ϕ_0	k_0	Lower bound			Upper bound			Average		
		C_{pc}^∞	γ	K	C_{pc}^∞	γ	K	C_{pc}^∞	γ	K
0–10	0.01–0.1							6.39	0.77	1345.54
0–5	0.1–1							56.3	0.65	1214.95
5–10	0.1–1	3.45	0.51	1327.64	11.3	1.22	1359.55	6.65	0.88	1346.19
5–10	1–10	4.03	0.60	1345.57	6.91	1.00	1360.42	5.23	0.75	1353.45
10–15	0.1–1	1.95	0.46	1351.21	6.96	1.55	1366.99	4.16	0.85	1359.88
10–15	1–10	2.29	0.49	1353.21	5.71	1.21	1366.68	3.55	0.78	1362.23
10–15	10–100	2.52	0.59	1356.25	5.07	1.11	1365.26	3.98	0.85	1360.39
15–20	1–10	1.69	0.46	1363.36	3.52	1.04	1367.85	2.81	0.78	1365.26
15–20	10–100	2.50	0.78	1362.90	3.86	1.16	1366.16	3.01	0.88	1364.95
20–25	10–100	1.45	0.54	1362.14	4.21	1.43	1368.83	2.82	1.01	1365.68

*Units: C_{pc}^∞ [$\times 10^{-6}$ psi $^{-1}$], γ and ϕ_0 [%], k_0 [mD], and K [psi]

data points showing a coefficient of determination (R^2) 97.12%. A similar effectiveness of the trendline were achieved for all of the rock core samples in the study with the coefficients of determination greater than 96% (Table 5). The remarkable consistency the exponential best fit for the variety of the corresponding experimental data tends to support the validity of Eq. (1) to represent the PVC versus stress relation. This proved exponential decay shows that the pore volume compressibility decreases as stress increases for all rock sample, while, the changes in the pore compressibility are greater at lower stresses, and as the stress increases, the amount of changes in pore compressibility are lower.

To evaluate the sensitivity of PVC to stress level, it is appropriate to calculate the percentage of the variation of PVC using the Eq. (1) as follows:

$$\% \Delta C_{pc} = \frac{\Delta C_{pc}}{C_{pc}} = \frac{1}{C_{pc}} \frac{dC_{pc}}{d\sigma} \Delta\sigma = -\frac{1}{K} \left(1 - \frac{C_{pc}^\infty}{C_{pc}} \right) \Delta\sigma \quad (2)$$

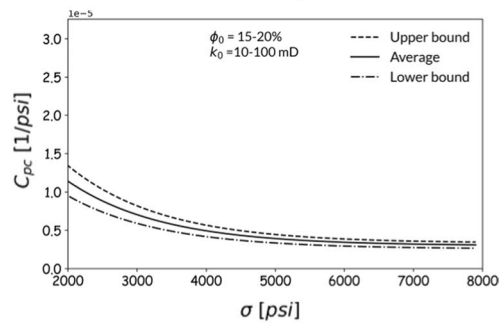
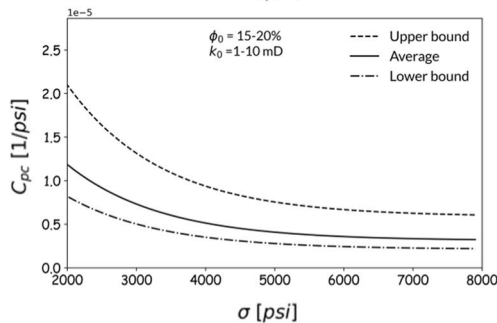
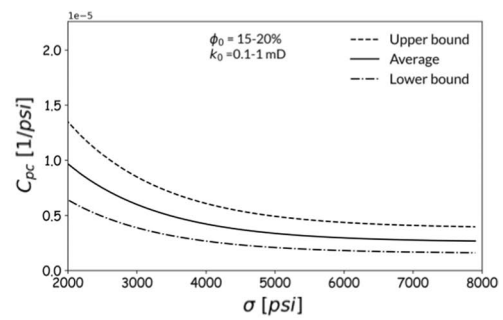
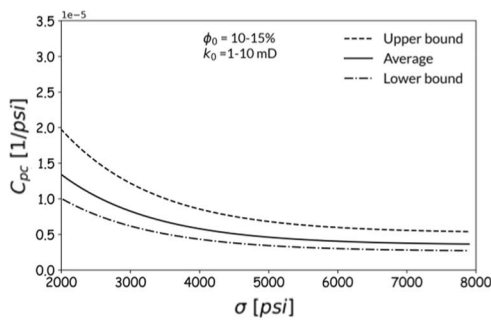
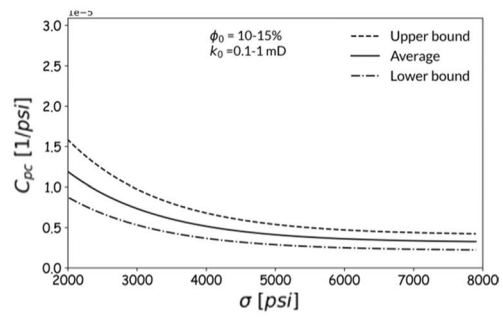
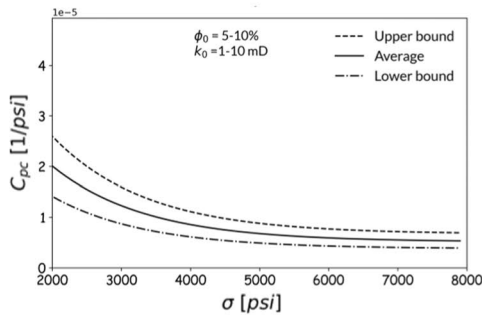
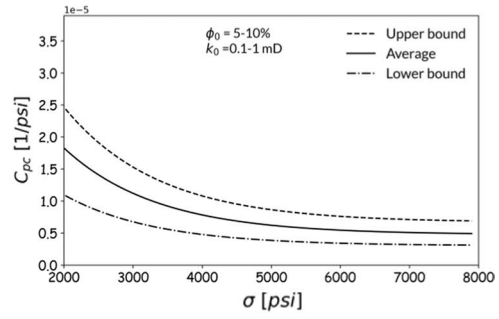
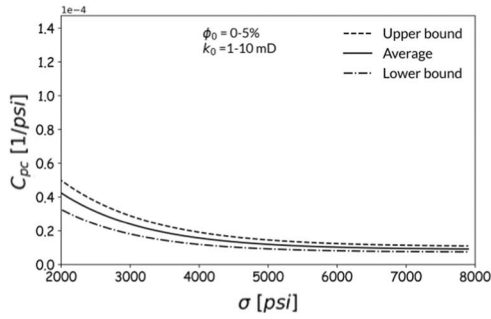
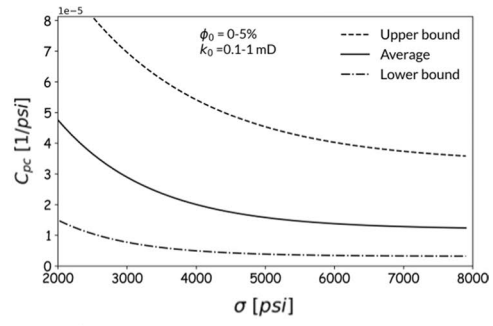
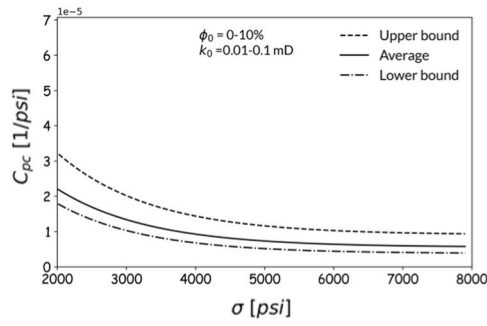
where $\% \Delta C_{pc}$ is the percentage of PVC variation that defines the ratio of the PVC variation to the PVC. This variable depends on C_{pc}^∞ and K coefficients as well as the value of PVC. As PVC decreases (or stress increases), the stress sensitivity of PVC decreases as well. As an example, for core sample No. 91 (Table 2), the percentage of the variation of PVC is 54% for stress change from 2000 to 3000 psi ($\Delta\sigma = 1000$ psi). While in the case of stress change

from 4000 to 5000 psi ($\Delta\sigma = 1000$ psi), this value is equal to 29%. Then, this sensitivity analysis has indicated the importance of having stress-dependent PVC, especially at each level of low-stress regimes.

This significant dependence of the PVC on stress indicates the importance of providing compressibility in reservoir studies as a function of stress instead of a constant value. In other words, using a constant value in reservoir engineering studies can cause a lot of errors.

4 Results and Discussion

To analyse the validity and accuracy of the empirical model based on the theory developed by Liu et al. (2009), the experimentally obtained results were compared to the trendline curve from Eq. (1). In all 200 core samples, the trendline was quite satisfactory with the coefficient of determination (R^2) greater than 0.97, reflecting the high validity and accuracy of the mathematical model. While various researchers proposed power law equations instead, the exponential Eq. (1) and the power-law regression were compared. The present study has shown that the exponential Eq. (1) is more accurate than the power-law formula. Moreover, the power-law regression model has no theoretical background. Also, the lack of interpretability is another problem related to this equation for the PVC–stress curve fitting. At the lower



◀**Fig. 5** The PVC–stress curves for limestone samples based on the classification of porosity–permeability frequent groups

stress levels, the difference between the experimental results and the power-law regression is dramatically increased because of a vertical asymptotic of the curve while confining stress approaches to zero, mathematically. However, such a situation does not occur in the case of using the exponential equation.

The values of the coefficients associated with the theoretical trendline between PVC and stress for different frequent porosity–permeability classes were shown in Table 3 for the limestones and in Table 4 for dolostones. For each of the coefficients, the average value and the lower and upper bounds were presented. This bandwidth provides a powerful tool to determine the limits of parametric effects in the reservoir models. The upper and lower bounds were obtained from each category's upper and lower PVC–stress curves. In contrast, while the average values were obtained from the arithmetic mean of the corresponding values. Figure 5 represents the plots of values in Table 3 for the limestones, and Fig. 6 shows these plots for dolostones as listed in Table 4.

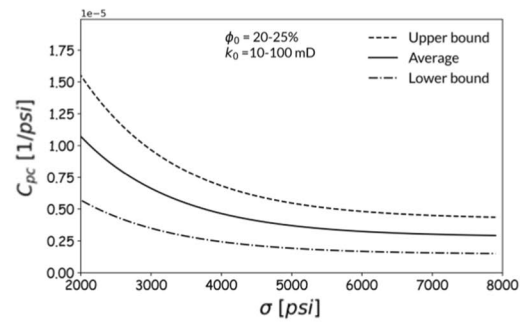
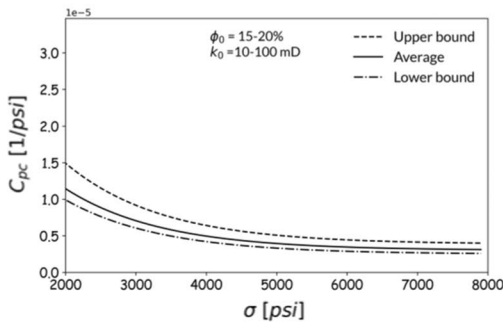
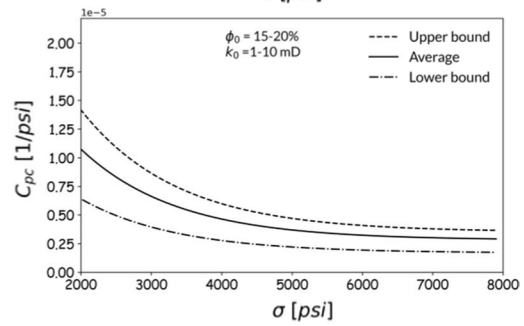
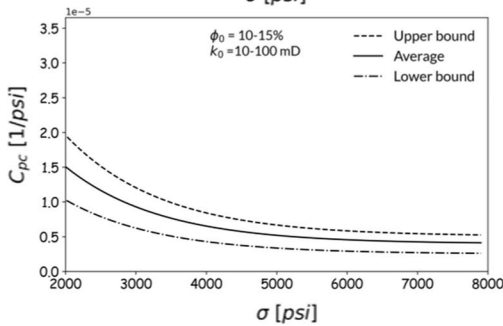
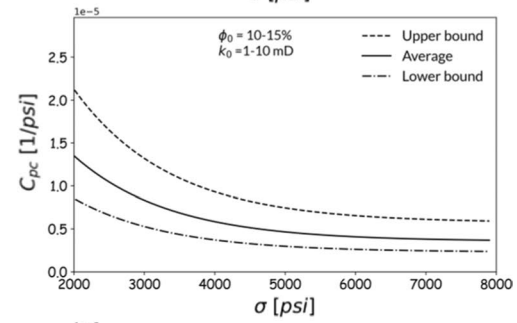
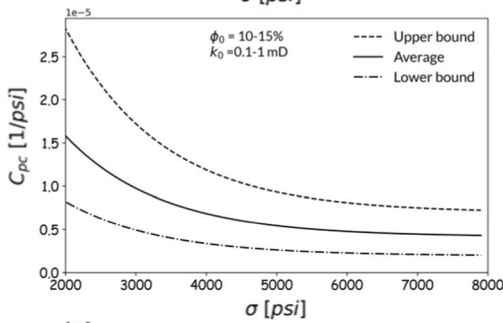
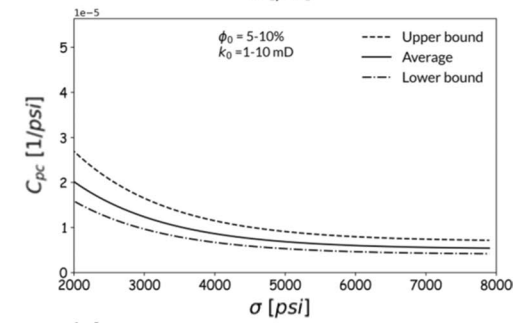
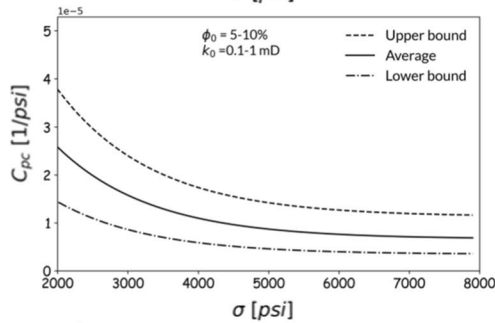
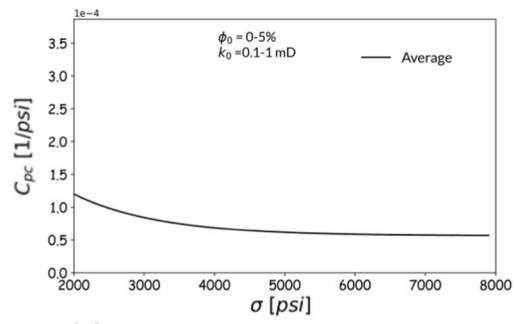
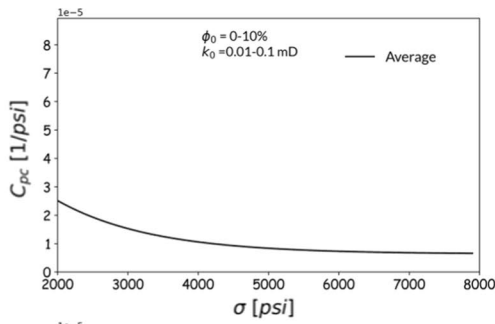
Furthermore, to turn the attention to the validity of the proposed model for prediction where the experimental PVC–stress data is not available, 12 random samples were collected with porosity–permeability in the range of the frequent categories and three out-of-range data. The experimental data from the PVC test have shown the acceptance of the proposed estimation curves for both in-range and out-of-range

core samples. The results are shown in Fig. 7 for the 12 in-range. Adjacent cells in cross-plot were used to estimate the coefficients of PVC–stress curve for data whose porosity–permeability was outside the frequency ranges. Figure 8 presents the prediction curves and the experimental data for these three core samples. The results have indicated that the proposed estimations are applicable over most of the range of experimental or in-situ accessible porosity and permeability data.

In the application of reservoir modelling it is useful to determine the representative elementary volume (REV) for the model, and based on the corresponding porosity and permeability profile in REV, the average values of porosity and permeability can be utilized to implement the correlated PVC–stress curve for each REVs.

5 Summary and Conclusion

The PVC literature abounds with tributes to the empirical PVC–porosity relation. But only in the last few years has special attention been paid to the importance of having PVC–stress relation. Therefore, due to the significance of the stress effect on PVC and the importance of having correlation to estimate the relationship in the case of no experimental PVC–stress data, we have combined petrographical and laboratory studies to achieve the goal. First, we have discussed the complexity of common geological categorizations based on pore structural inspection of



◀**Fig. 6** The PVC–stress curves for dolostone samples based on the classification of porosity–permeability frequent groups

thin sections for this estimate. So, we have used the petrophysical properties of rock, including porosity and permeability, and also the lithological description of samples to find out the empirical–theoretical-based correlation between PVC and stress for different cases. Accordingly, several thin sections and previously gathered core data were studied for two important reservoir Formations of Iran: the Bangestan

group and Asmari. As the effect of geological pore structure complexity exhibited in the porosity and permeability of core samples, the most frequent porosity–permeability was chosen as a base for sample selection to perform PVC experimental tests; 200 core samples were tested and analyzed. Based on the pre-approved theoretical equation, the PVC–stress relations were quantified. This categorization for estimating the relation coefficients was well examined on 15 different core samples that were not involved in determining the coefficients.

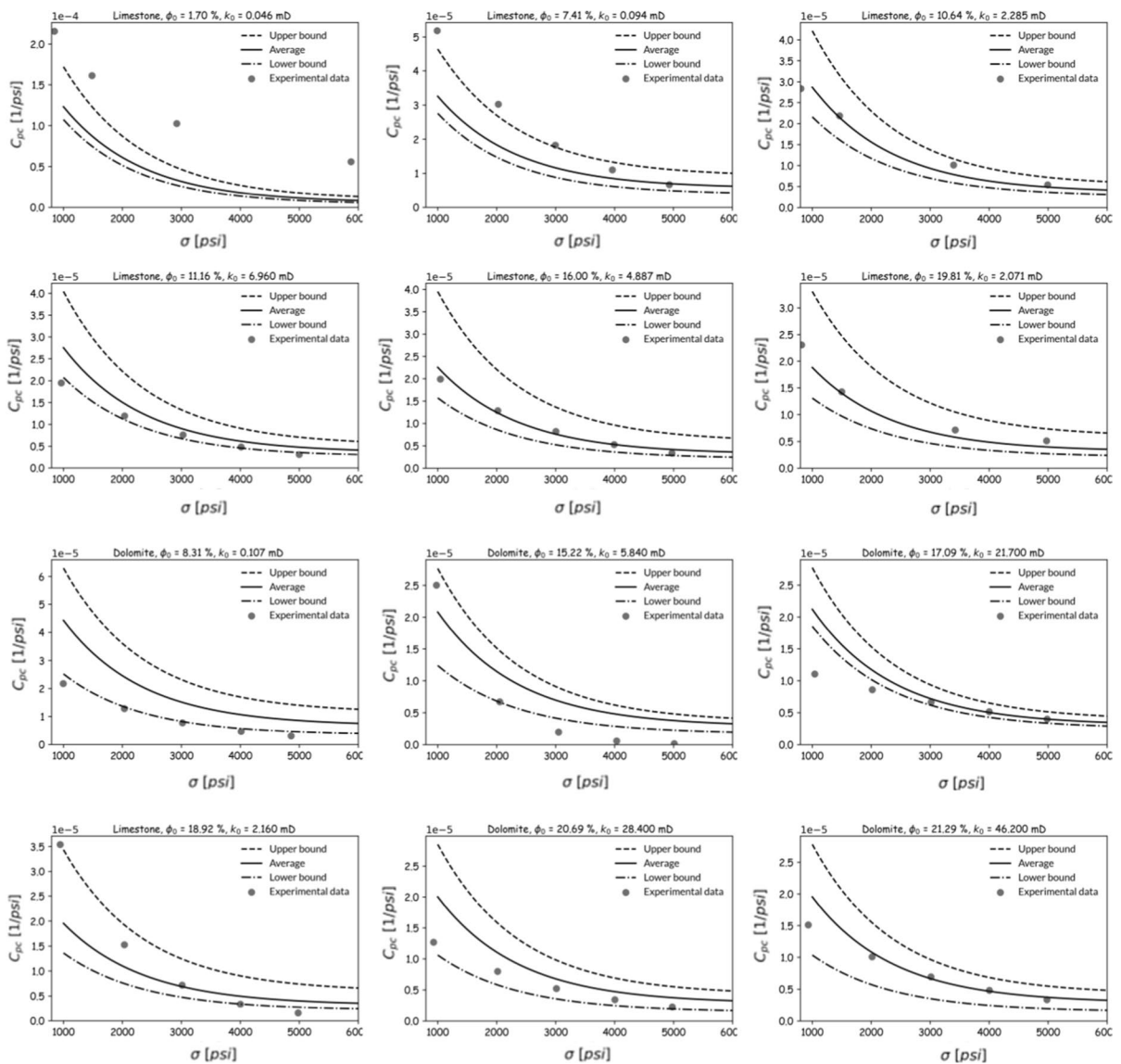


Fig. 7 Verification of the proposed correlation for limestone and dolostone samples based on the classification of porosity–permeability frequent groups for samples whose porosity–permeability are in the range of the frequent groups

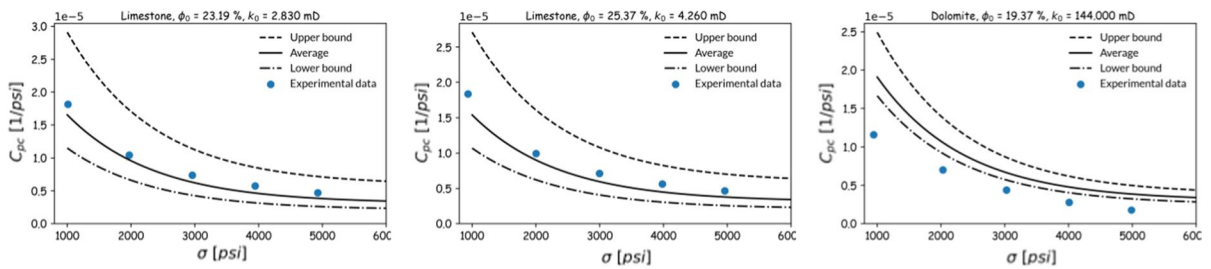


Fig. 8 Verification of the proposed correlation for limestone and dolomite samples based on the classification of porosity–permeability frequent groups for samples whose porosity–permeability are not in the range of the frequent groups

Furthermore, the present experimental study has even proved the validity of the theoretical exponential relationship between PVC and stress which has been proposed by Liu et al. (2009). We have shown that the equation is useful for understanding the effect of reservoir production on volumetric change of pores. It has demonstrated that the sensitivity of PVC to stress is not ignorable, such as what was reported in the literature. So, dismissing the stress effect on PVC as a material property information of porous rock contained in reservoir modeling led to an error in the analysis. The sensitivity analysis of the equation revealed that changes in stress, significant changes occur in the value of PVC, especially at low-stress levels.

Funding The authors have not disclosed any funding.

Data availability Enquiries about data availability should be directed to the authors.

Declarations

Conflict of interest The authors have not disclosed any competing interests.

Appendix

See Table 5.

Table 5 Experimental data from core samples used to analyze the correlations

NO	Formation	Lithology	$\rho\left(\frac{\text{g}}{\text{cm}^3}\right)$	$k_{air}(md)$	$\phi_0(\%)$	$C_{pc}^\infty(\times 10^{-6}\text{psi}^{-1})$	$\gamma(\%)$	$K(\text{psi})$	R^2
1	AS	L	2.70	0.078	6.54	4.64	0.52	1352.80	0.9706
2	AS	DL	2.73	0.146	8.60	4.61	0.67	1354.91	0.9711
3	AS	DL	2.93	0.162	9.40	3.47	0.55	1360.39	0.9709
4	AS	SL	2.70	0.380	7.28	6.67	0.85	1342.95	0.9714
5	AS	L	2.72	0.198	10.89	3.40	0.62	1361.84	0.9710
6	AS	L	2.71	0.683	13.67	2.15	0.48	1366.36	0.9710
7	AS	L	2.72	0.534	12.56	4.07	0.86	1359.30	0.9712
8	AS	L	2.71	0.204	10.38	3.47	0.60	1361.17	0.9712
9	AS	L	2.72	0.682	14.37	2.46	0.58	1365.41	0.9712
10	AS	L	2.67	0.767	14.28	2.69	0.64	1364.96	0.9713
11	AS	L	2.72	0.165	1.73	33.02	0.35	1766.18	0.9800
12	AS	L	2.71	0.295	3.19	8.02	0.60	1266.38	0.9701
13	AS	DL	2.77	0.105	3.34	8.55	1.01	1251.39	0.9695
14	AS	L	2.71	0.467	4.17	10.80	0.97	1318.93	0.9709
15	AS	L	2.72	0.585	4.20	7.92	0.64	1337.74	0.9706
16	AS	DL	2.76	1.666	15.20	2.45	0.62	1365.95	0.9706
17	AS	L	2.81	2.125	15.84	2.77	0.73	1365.02	0.9709
18	AS	L	2.71	1.341	17.03	2.65	0.75	1365.61	0.9712
19	AS	DL	2.73	4.131	16.70	3.21	0.89	1364.17	0.9708
20	AS	L	2.74	5.485	18.09	2.12	0.63	1366.71	0.9710
21	AS	DL	2.73	2.631	14.70	3.19	0.78	1363.80	0.9713
22	AS	DL	2.75	12.892	12.69	3.60	0.76	1361.52	0.9709
23	AS	L	2.81	10.405	13.51	7.47	1.76	1345.89	0.9712
24	AS	DL	2.75	1.288	11.98	3.08	0.61	1362.65	0.9709
25	AS	L	2.71	9.993	14.89	3.74	0.93	1363.16	0.9711
26	AS	L	2.71	1.003	13.99	3.08	0.71	1364.13	0.9705
27	AS	L	2.71	1.705	4.73	10.53	0.96	1310.80	0.9713
28	AS	L	2.72	4.292	8.11	4.42	0.61	1354.11	0.9719
29	AS	L	2.69	46.248	18.00	2.89	0.86	1365.08	0.9709
30	AS	L	2.71	173.237	20.48	4.05	1.38	1362.66	0.9711
31	AS	L	2.72	495.190	24.01	3.59	1.43	1364.44	0.9713
32	AS	L	2.71	37.156	20.67	3.21	1.10	1364.95	0.9712
33	Bg	L	2.71	0.086	6.78	4.26	0.49	1353.97	0.9712
34	Bg	L	2.72	0.069	5.38	5.31	0.51	1335.08	0.9721
35	Bg	L	2.70	0.099	8.46	3.80	0.54	1358.98	0.9714
36	Bg	L	2.72	0.037	3.20	9.07	0.79	1286.67	0.9712
37	Bg	L	2.71	0.046	3.99	6.48	0.53	1311.66	0.9711
38	Bg	L	2.69	0.470	2.69	6.81	0.34	1359.00	0.9647
39	Bg	L	2.69	0.103	4.37	9.06	0.78	1327.11	0.9720
40	Bg	DL	2.70	0.325	3.92	12.28	1.13	1266.38	0.9694
41	Bg	L	2.72	0.485	2.38	33.44	0.28	1799.10	0.9698
42	Bg	L	2.70	0.433	4.55	11.86	1.18	1289.20	0.9707
43	Bg	L	2.69	0.713	2.44	3.20	0.92	1056.50	0.9668
44	Bg	L	2.71	0.152	3.31	7.15	0.51	1323.22	0.9703
45	Bg	L	2.71	0.123	4.91	7.42	0.70	1308.30	0.9710

Table 5 (continued)

NO	Formation	Lithology	$\rho\left(\frac{\text{g}}{\text{cm}^3}\right)$	$k_{air}(md)$	$\phi_0(\%)$	$C_{pc}^\infty(\times 10^{-6}\text{psi}^{-1})$	$\gamma(\%)$	$K(\text{psi})$	R^2
46	Bg	L	2.72	1.038	3.20	8.57	0.88	1168.92	0.9679
47	Bg	L	2.72	0.267	2.88	8.04	0.74	1211.72	0.9698
48	Bg	DL	2.71	1.064	3.40	7.32	0.66	1227.86	0.9704
49	Bg	L	2.72	0.343	7.53	3.04	0.38	1360.84	0.9706
50	Bg	L	2.71	0.429	9.35	5.39	0.86	1354.25	0.9709
51	Bg	L	2.56	0.788	6.00	5.81	0.60	1324.06	0.9714
52	Bg	L	2.69	0.309	7.55	3.72	0.47	1335.86	0.9726
53	Bg	L	2.72	0.108	6.93	5.29	0.63	1349.76	0.9711
54	Bg	L	2.69	0.566	6.04	5.86	0.62	1344.25	0.9708
55	Bg	L	2.66	0.212	8.11	5.94	0.83	1349.72	0.9716
56	Bg	L	2.70	0.183	8.91	5.43	0.83	1353.38	0.9716
57	Bg	L	2.70	0.983	8.66	3.53	0.51	1360.01	0.9710
58	Bg	DL	2.69	0.136	9.67	4.33	0.71	1358.45	0.9716
59	Bg	L	2.71	0.435	8.76	4.19	0.62	1357.96	0.9711
60	Bg	L	2.71	0.230	7.63	4.12	0.53	1355.06	0.9707
61	Bg	L	2.70	0.155	9.89	4.19	0.70	1357.23	0.9713
62	Bg	L	2.70	0.711	6.67	5.43	0.63	1348.25	0.9714
63	Bg	L	2.52	1.081	8.79	5.88	0.89	1351.42	0.9726
64	Bg	L	2.69	1.398	8.38	6.70	0.98	1346.30	0.9709
65	Bg	L	2.70	1.962	8.52	3.81	0.54	1359.31	0.9712
66	Bg	L	2.69	5.983	4.81	9.09	0.84	1307.98	0.9704
67	Bg	L	2.70	1.792	9.60	4.20	0.68	1358.89	0.9713
68	Bg	DL	2.73	1.548	9.92	5.98	1.01	1353.17	0.9713
69	Bg	L	2.72	2.656	13.16	2.63	0.57	1364.88	0.9710
70	Bg	L	2.71	2.320	12.44	2.93	0.60	1363.73	0.9706
71	Bg	L	2.71	2.197	12.51	3.76	0.79	1361.01	0.9707
72	Bg	L	2.69	1.091	10.80	4.16	0.76	1357.50	0.9701
73	Bg	L	2.69	1.229	10.44	4.02	0.71	1359.54	0.9716
74	Bg	L	2.69	1.440	12.70	5.21	1.12	1357.07	0.9710
75	Bg	L	2.70	1.180	14.86	3.12	0.77	1364.35	0.9711
76	Bg	DL	2.70	2.361	13.78	3.40	0.78	1363.28	0.9711
77	Bg	DL	2.72	0.167	12.66	2.96	0.62	1363.83	0.9714
78	Bg	L	2.71	0.980	12.89	2.88	0.62	1364.19	0.9711
79	Bg	L	2.70	0.978	10.89	3.55	0.65	1361.49	0.9713
80	Bg	DL	2.72	0.727	15.66	3.85	1.01	1362.30	0.9713
81	Bg	L	2.69	0.313	13.31	2.83	0.62	1364.44	0.9713
82	Bg	L	2.64	0.294	11.89	3.73	0.74	1360.88	0.9716
83	Bg	L	2.71	0.267	10.99	3.50	0.64	1361.71	0.9710
84	Bg	L	2.70	16.367	13.34	5.29	1.19	1356.72	0.9705
85	Bg	L	2.69	6.651	22.32	2.99	1.10	1365.36	0.9711
86	Bg	L	2.70	8.225	25.89	3.44	1.48	1364.67	0.9710
87	Bg	L	2.69	2.449	16.71	3.04	0.84	1364.73	0.9710
88	Bg	L	2.69	6.174	17.84	2.96	0.87	1365.16	0.9711
89	Bg	L	2.70	4.109	19.22	2.47	0.78	1366.43	0.9711
90	Bg	DL	2.69	1.256	18.84	3.61	1.13	1363.76	0.9711

Table 5 (continued)

NO	Formation	Lithology	$\rho\left(\frac{\text{g}}{\text{cm}^3}\right)$	$k_{air}(md)$	$\phi_0(\%)$	$C_{pc}^\infty(\times 10^{-6}\text{psi}^{-1})$	$\gamma(\%)$	$K(\text{psi})$	R^2
91	Bg	DL	2.72	0.708	17.46	3.11	0.90	1364.65	0.9712
92	Bg	DL	2.70	1.185	15.43	5.87	1.53	1356.88	0.9711
93	Bg	L	2.70	1.203	20.00	2.73	0.90	1365.93	0.9711
94	Bg	L	2.70	1.409	17.57	3.28	0.96	1364.35	0.9711
95	Bg	L	2.70	1.550	15.94	2.90	0.76	1364.99	0.9709
96	Bg	DL	2.71	1.958	15.00	3.52	0.88	1363.22	0.9710
97	Bg	DL	2.72	3.844	15.79	3.26	0.85	1364.06	0.9711
98	Bg	DL	2.71	7.196	17.05	3.54	1.00	1363.61	0.9710
99	Bg	L	2.70	13.097	24.96	5.31	2.23	1360.37	0.9708
100	Bg	L	2.68	12.735	17.76	2.58	0.76	1366.09	0.9706
NO	Formation	Lithology	$\rho\left(\frac{\text{g}}{\text{cm}^3}\right)$	$k_{air}(md)$	$\phi_0(\%)$	$C_{pc}^\infty(\times 10^{-6}\text{psi}^{-1})$	$\gamma(\%)$	$K(\text{psi})$	R^2
101	Bg	L	2.67	55.370	19.96	3.33	1.10	1364.65	0.9710
102	Bg	L	2.69	17.254	18.20	3.17	0.95	1364.82	0.9711
103	Bg	L	2.67	0.148	19.72	1.57	0.51	1368.13	0.9708
104	Bg	L	2.67	0.104	17.95	1.85	0.55	1367.53	0.9720
105	Bg	L	2.72	28.259	29.16	4.24	2.05	1363.42	0.9718
106	Bg	L	2.71	16.828	27.03	2.86	1.28	1366.08	0.9711
107	Bg	L	2.70	2.207	22.91	3.05	1.16	1365.14	0.9712
108	Bg	L	2.71	51.200	27.76	3.88	1.79	1364.20	0.9712
109	Bg	L	2.70	3.299	26.12	2.70	1.16	1366.57	0.9717
110	AS	D	2.83	0.075	6.93	6.39	0.77	1345.54	0.9712
111	AS	D	2.87	3.684	14.94	2.57	0.63	1365.45	0.9714
112	AS	D	2.85	1.012	12.78	2.80	0.59	1364.29	0.9707
113	AS	LD	2.81	2.633	12.36	2.48	0.51	1364.43	0.9709
114	AS	LD	2.81	3.412	11.99	4.00	0.80	1360.34	0.9709
115	AS	LD	2.80	2.988	14.76	3.47	0.85	1362.90	0.9703
116	AS	LD	2.73	1.580	11.93	3.43	0.68	1362.25	0.9707
117	AS	LD	2.80	2.190	14.05	2.63	0.61	1364.71	0.9707
118	AS	D	2.88	1.244	14.17	3.62	0.86	1361.90	0.9710
119	AS	D	2.82	7.228	12.15	5.71	1.18	1353.21	0.9708
120	AS	D	2.82	1.448	10.23	4.70	0.81	1358.43	0.9708
121	AS	D	2.85	4.821	14.62	2.91	0.70	1364.71	0.9707
122	AS	SD	2.76	4.008	14.00	5.15	1.21	1358.54	0.9709
123	AS	D	2.87	4.296	14.24	4.80	1.15	1358.31	0.9710
124	AS	D	2.85	4.523	13.91	2.29	0.52	1366.68	0.9707
125	AS	DS/SD	2.72	2.261	14.42	3.58	0.86	1363.92	0.9709
126	AS	D	2.85	1.643	11.72	2.53	0.49	1365.72	0.9707
127	AS	D	2.87	0.169	8.52	7.24	1.07	1344.39	0.9708
128	AS	LD	2.81	0.112	5.32	11.29	1.18	1327.64	0.9703
129	AS	LD	2.77	0.160	7.37	5.85	0.75	1349.01	0.9704
130	AS	SD/DS	2.73	0.124	6.02	6.39	0.69	1336.42	0.9716
131	AS	LD	2.81	0.189	7.19	4.99	0.61	1351.64	0.9704
132	AS	LD	2.75	0.156	5.97	4.93	0.51	1348.74	0.9703

Table 5 (continued)

NO	Formation	Lithology	$\rho\left(\frac{\text{g}}{\text{cm}^3}\right)$	$k_{air}(\text{md})$	$\phi_0(\%)$	$C_{pc}^\infty(\times 10^{-6}\text{psi}^{-1})$	$\gamma(\%)$	$K(\text{psi})$	R^2
133	AS	D	2.82	0.114	9.54	4.01	0.65	1358.44	0.9713
134	AS	D	2.85	0.803	9.72	5.70	0.95	1351.88	0.9715
135	AS	D	2.88	0.778	9.58	3.45	0.56	1359.55	0.9707
136	AS	SD	2.75	0.534	7.25	9.21	1.20	1332.74	0.9706
137	AS	D	2.89	0.102	6.15	8.11	0.91	1355.37	0.9705
138	AS	D	2.87	0.602	9.69	7.22	1.22	1344.81	0.9704
139	AS	LD	2.80	0.276	8.58	8.02	1.22	1339.80	0.9703
140	AS	D	2.81	0.696	17.23	2.81	0.80	1365.38	0.9715
141	AS	D	2.84	0.404	13.44	3.92	0.88	1361.94	0.9709
142	AS	LD	2.80	0.348	10.53	5.82	1.05	1353.49	0.9710
143	AS	D	2.84	0.811	11.41	3.06	0.58	1362.73	0.9705
144	AS	D	2.85	0.515	14.25	1.95	0.46	1366.99	0.9712
145	AS	D	2.82	0.146	12.35	2.75	0.56	1364.32	0.9708
146	AS	D	2.87	0.812	12.01	3.94	0.80	1359.59	0.9711
147	AS	D	2.80	0.157	14.69	2.20	0.53	1366.36	0.9711
148	AS	D	2.82	0.396	15.96	2.90	0.76	1364.85	0.9712
149	AS	D	2.79	0.610	12.96	6.96	1.55	1351.21	0.9707
150	AS	LD	2.80	0.532	10.05	4.19	0.71	1357.61	0.9709
151	AS	D	2.81	0.403	14.52	4.05	0.99	1360.87	0.9707
152	AS	D	2.82	0.169	11.23	5.05	0.96	1356.87	0.9713
153	AS	LD	2.74	0.955	12.00	5.31	1.08	1357.59	0.9713
154	AS	LD	2.76	0.849	11.61	5.96	1.18	1354.47	0.9710
155	AS	D	2.83	0.395	10.64	3.63	0.64	1362.41	0.9713
156	AS	D	2.83	0.970	16.97	2.98	0.84	1364.95	0.9710
157	AS	D	2.81	0.879	19.60	2.38	0.77	1366.64	0.9706
158	AS	D	2.84	7.139	15.55	1.81	0.46	1367.49	0.9711
159	AS	LD	2.80	3.456	17.23	1.69	0.48	1367.85	0.9708
160	AS	D	2.63	2.744	20.87	1.91	0.65	1367.83	0.9717
161	AS	D	2.83	3.991	15.19	2.61	0.65	1365.32	0.9709
162	AS	D	2.85	6.204	15.64	3.35	0.87	1363.40	0.9706
163	AS	D	2.83	2.433	20.78	2.18	0.75	1367.09	0.9711
164	AS	D	2.86	4.579	17.19	3.33	0.95	1363.71	0.9708
165	AS	D	2.85	2.728	17.87	3.52	1.04	1363.36	0.9706
166	AS	SD	2.80	5.722	17.80	3.19	0.94	1364.47	0.9705
167	AS	D	2.80	2.793	20.79	5.03	1.75	1361.09	0.9713
168	AS	D	2.82	1.641	16.27	2.52	0.68	1365.98	0.9711
169	AS	LD	2.79	3.199	16.08	2.45	0.65	1366.59	0.9709
170	AS	D	2.81	4.048	15.85	2.88	0.75	1365.52	0.9709
171	AS	SD	2.72	5.909	15.14	2.43	0.61	1366.63	0.9709
172	AS	D	2.82	6.467	18.24	3.32	1.00	1364.59	0.9706
173	AS	D	2.81	3.202	7.36	5.68	0.72	1350.02	0.9707
174	AS	D	2.85	3.204	8.95	4.53	0.68	1356.45	0.9711
175	AS	D	2.84	1.976	8.86	5.00	0.75	1354.82	0.9706
176	AS	D	2.87	1.209	8.33	6.91	1.00	1345.57	0.9710
177	AS	D	2.85	4.535	8.86	4.03	0.60	1360.42	0.9714

Table 5 (continued)

NO	Formation	Lithology	$\rho\left(\frac{\text{g}}{\text{cm}^3}\right)$	$k_{air}(\text{md})$	$\phi_0(\%)$	$C_{pc}^\infty(\times 10^{-6}\text{psi}^{-1})$	$\gamma(\%)$	$K(\text{psi})$	R^2
178	AS	D	2.84	13.904	18.18	2.71	0.81	1366.07	0.9704
179	AS	D	2.85	19.811	18.89	2.50	0.78	1366.16	0.9706
180	AS	D	2.84	10.120	15.81	2.99	0.78	1364.65	0.9709
181	AS	D	2.87	66.063	22.57	1.45	0.54	1368.83	0.9710
182	AS	D	2.84	128.197	26.61	2.11	0.92	1367.68	0.9712
183	AS	D	2.85	111.660	23.80	2.79	1.10	1366.00	0.9710
184	AS	D	2.85	71.032	20.33	1.82	0.61	1367.84	0.9709
185	AS	LD	2.87	18.919	24.26	3.53	1.42	1364.14	0.9710
186	AS	D	2.89	10.640	20.38	4.21	1.43	1362.14	0.9706
187	AS	D	2.86	46.776	21.68	2.85	1.02	1365.96	0.9707
188	AS	D	2.86	23.419	20.38	3.44	1.16	1363.81	0.9709
189	AS	D	2.83	12.175	26.04	2.41	1.03	1367.22	0.9706
190	AS	D	2.82	10.219	20.24	2.45	0.82	1367.04	0.9709
191	AS	LD	2.81	0.114	1.63	56.34	0.65	1214.95	0.9708
192	AS	D	2.85	13.422	14.26	2.52	0.59	1365.26	0.9908
193	AS	D	2.83	12.787	10.61	4.55	0.81	1358.05	0.9709
194	AS	D	2.84	13.603	13.75	3.78	0.87	1361.99	0.9711
195	AS	D	2.86	12.249	12.89	5.07	1.11	1356.25	0.9713
196	AS	D	2.84	7.935	24.14	2.25	0.90	1367.18	0.9707
197	Bg	LD	2.75	2.279	12.63	3.64	0.77	1362.08	0.9710
198	Bg	LD	2.69	0.396	12.64	3.62	0.76	1361.78	0.9706
199	Bg	LD	2.76	5.611	17.58	3.52	1.03	1363.49	0.9711
200	Bg	D	2.72	12.029	18.06	3.86	1.16	1362.90	0.9707

AS. Asmari, Bg. Bangestan, D dolomite, L limestone, SD sandy/silty dolomite, DS dolomitic siltstone/sandstone, DL dolomitic limestone, LD limy dolostone

References

- Aloki Bakhtiari H, Moosavi A, Kazemzadeh E, Goshtasbi K, Esfahani MR, Vali J (2011). Geopersia 1(1):37–82
- Aloki Bakhtiari H, Moosavi SA, Honarmand MJ (2014) Research Project Report: Compressibility of the Asmari and Bangestan reservoir rocks in Gachsaran, Bibihakimeh, Ragsefid, Aghajari and Maroon, (Contract No. 0226-21-86): Client: National Iranian South Oil Company.
- Archie GE (1952) Classification of carbonate reservoir rocks and petrophysical considerations*. AAPG Bull 36(2):278–298.
- Choquette PW, Pray LC (1970) Geologic nomenclature and classification of porosity in sedimentary carbonates. AAPG Bull 54(2):207–250
- Chuanliang L, Xiaofan C, Zhimin D (2004) A New relationship of rock compressibility with porosity: SPE Asia Pacific oil and gas conference and exhibition. APOGCE.
- da Silva GP, Franco DR, Stael GC, da Costa de Oliveira Lima M, Sant'Anna Martins R, de Moraes França O, Azeredo RBV (2015) Petrophysical studies of north American carbonate rock samples and evaluation of pore-volume compressibility models. J Appl Geophys 123:256–266
- Dou Q, Sun Y, Sullivan C (2011) Rock-physics-based carbonate pore type characterization and reservoir permeability heterogeneity evaluation, Upper San Andres reservoir, Permian Basin, west Texas. J Appl Geophys 74(1):8–18
- Geertsma J (1957) The effect of fluid pressure decline on volumetric changes of porous rocks. Trans AIME 210(01):331–340
- Hall HN (1953) Compressibility of reservoir rocks. J Petrol Technol 5(01):17–19
- Harari Z, Shu-Teh W, Salih S (1995) Pore-compressibility study of Arabian Carbonate reservoir rocks. SPE Form Eval 10(04):207–214
- Horne RN (1997) Modern well test analysis: a computer-aided approach, Petroway.
- Jalalh AA (2006a) Compressibility of porous rocks: Part I. Measurements of Hungarian reservoir rock samples. Acta Geophys 54(3):319–332.
- Jalalh AA (2006b) Compressibility of porous rocks: Part II. New Relationships Acta Geophys 54(4):399–412
- Lei G, Cao N, McPherson BJ, Liao Q, Chen W (2019) A novel analytical model for pore volume compressibility of fractal porous media. Sci Rep 9(1):14472

- Lis-Śledziona A (2019) Petrophysical rock typing and permeability prediction in tight sandstone reservoir. *Acta Geophys* 67(6):1895–1911
- Liu H-H, Rutqvist J, Berryman J (2009) On the relationship between stress and elastic strain for fractured rock. *Int J Rock Mech Min Sci* 46:289–296
- Liu H-H, Lai B, Chen J, Georgi D (2016) Pressure pulse-decay tests in a dual-continuum medium: late-time behavior. *J Petrol Sci Eng*, vol 147.
- Lucia FJ (1983) Petrophysical parameters estimated from visual descriptions of carbonate rocks: a field classification of carbonate pore space. *J Petrol Technol* 35(03):629–637
- Moosavi SA, Goshtasbi K, Kazemzadeh E, Bakhtiari HA, Esfahani MR, Vali J (2014) Relationship between porosity and permeability with stress using pore volume compressibility characteristic of reservoir rocks. *Arab J Geosci* 7(1):231–239
- Murray RC (1960) Origin of porosity in carbonate rocks. *J Sediment Res* 30(1):59–84
- Newman GH (1973) Pore-volume compressibility of consolidated, friable, and unconsolidated reservoir rocks under hydrostatic loading. *J Petrol Technol* 25(02):129–134
- Oliveira GLP, Ceia MAR, Missagia RM, Archilha NL, Figueiredo L, Santos VH, Lima Neto I (2016) Pore volume compressibilities of sandstones and carbonates from Helium porosimetry measurements. *J Petrol Sci Eng* 137:185–201
- Rinaldi AP, Rutqvist J (2019) Joint opening or hydroshearing? Analyzing a fracture zone stimulation at Fenton Hill. *Geothermics* 77:83–98
- Satter A, Iqbal GM (2016) 3-Reservoir rock properties. In: Satter A, Iqbal GM (eds) *Reservoir engineering*. Gulf Professional Publishing, Boston, pp 29–79.
- El Sawy MZ, Abuhagaza AA, Nabawy BS, Lashin A (2020) Rock typing and hydraulic flow units as a successful tool for reservoir characterization of Bentiu-Abu Gabra sequence, Muglad basin, southwest Sudan. *J African Earth Sci* 171:103961.
- Sui W, Quan Z, Hou Y, Cheng H (2020) Estimating pore volume compressibility by spheroidal pore modeling of digital rocks. *Pet Explor Dev* 47(3):603–612
- Teeuw D (1971) Prediction of formation compaction from laboratory compressibility data. *Soc Petrol Eng J* 11(03):263–271
- van der Knaap W (1959) Nonlinear behavior of elastic porous media. *Trans AIME* 216(01):179–187
- Wang X-S, Jiang X-W, Wan L, Song G, Xia Q (2009) Evaluation of depth-dependent porosity and bulk modulus of a shear using permeability–depth trends. *Int J Rock Mech Min Sci* 46(7):1175–1181
- Zheng X, Espinoza DN (2021) Measurement of unloading pore volume compressibility of frio sand under uniaxial strain stress path and implications on reservoir pressure management. *Rock Mech Rock Eng* 54:5745–5760
- Zheng J, Ju Y, Liu H-H, Zheng L, Wang M (2016) Numerical prediction of the decline of the shale gas production rate with considering the geomechanical effects based on the two-part Hooke's model. *Fuel* 185:362–369
- Zhu S, Du Z, Li C, You Z, Peng X, Deng P (2018) An analytical model for pore volume compressibility of reservoir rock. *Fuel* 232:543–549
- Zimmerman RW (1991) *Compressibility of sandstones*. Elsevier, Amsterdam

Publisher's Note Springer Nature remains neutral with regard to jurisdictional claims in published maps and institutional affiliations.